The Canadian Mineralogist
Vol. 38, pp. 1425-1432 (2000)

REFINEMENT OF THE CRYSTAL STRUCTURE OF VÄYRYNENITE

DANIELLE M.C. HUMINICKI AND FRANK C. HAWTHORNE§

Department of Geological Sciences, University of Manitoba, Winnipeg, Manitoba R3T 2N2, Canada

ABSTRACT

Väyrynenite, $(Mn^{2+}_{0.78}Fe^{2+}_{0.23}Mg_{0.01})Be(PO_4)(OH_{0.92}F_{0.08})$, is monoclinic, *a* 5.4044(6), *b* 14.5145(12), *c* 4.7052(6) Å, β 102.798(9)°, *V* 359.91(7) Å^3, space group $P2_1/a$, $Z = 4$. The structure was refined to an *R* index of 1.5% based on 1001 observed [$|F_o| > 5\sigma F$] for reflections measured with Mo$K\alpha$ X-radiation using a single-crystal diffractometer. In the structure of väyrynenite, (Beφ_4) tetrahedra connect to adjacent (Beφ_4) tetrahedra by corner-sharing of anions in a zigzag pattern to form a chain that extends in the *a* direction. This chain is decorated along its periphery by (PO_4) tetrahedra that corner-share with one O atom from each of two different (Beφ_4) tetrahedra to form ribbons along the *c* axis. These $[Be_2(OH)_2(PO_4)_2]_n^{4n-}$ ribbons, which somewhat resemble the $[Be_2(OH)_2(SiO_4)_2]$ chains in euclase, $AlBe(SiO_4)(OH)$, are linked in the *b* direction by (Mn^{2+},Fe^{2+}) in octahedral coordination. The resultant (001) sheets are linked to adjacent sheets in the *c* direction by corner-sharing of O atoms between (PO_4) tetrahedra and {(Mn,Fe)φ_6}octahedra, and by hydrogen bonds. The hydrogen position was determined directly, and a sensible hydrogen-bonding scheme established. The connectivity of the (Beφ_4–$T\varphi_4$) (*T* = Si,P) chains in Be minerals is examined, and arranged in a hierarchy of increasing topological complexity.

Keywords: väyrynenite, crystal-structure refinement, electron-microprobe analysis, Be minerals.

SOMMAIRE

La väyrynenite, $(Mn^{2+}_{0.78}Fe^{2+}_{0.23}Mg_{0.01})Be(PO_4)(OH_{0.92}F_{0.08})$, est monoclinique, *a* 5.4044(6), *b* 14.5145(12), *c* 4.7052(6) Å, β 102.798(9)°, *V* 359.91(7) Å^3, groupe spatial $P2_1/a$, $Z = 4$. Nous avons affiné la structure jusqu'à un résidu *R* de 1.5% en utilisant 1001 réflexions observées [$|F_o| > 5\sigma F$] et mesurées avec rayonnement Mo$K\alpha$ et diffractométrie sur cristal unique. Dans la structure de la väyrynenite, les tétraèdres (Beφ_4) sont liés aux tétraèdres (Beφ_4) adjacents par partage d'anions pour former un agencement en zig-zag, la chaîne étant allongée dans la direction *a*. Cette chaîne est décorée dans ses parties périphériques par des tétraèdres (PO_4) qui partagent leurs coins avec un atome O, chacun provenant de deux tétraèdres (Beφ_4) différents, pour former des rubans le long de l'axe *c*. Ces rubans, de composition $[Be_2(OH)_2(PO_4)_2]_n^{4n-}$, qui ressemblent *grosso modo* aux chaînes $[Be_2(OH)_2(SiO_4)_2]$ dans l'euclase, $AlBe(SiO_4)(OH)$, sont liées dans la direction *b* par (Mn^{2+},Fe^{2+}) en coordinence octaédrique. Les feuillets (001) résultants sont liés aux feuillets voisins dans la direction *c* par partage des atomes O des coins entre les tétraèdres (PO_4) et les octaèdres {(Mn,Fe)φ_6}, et par liaisons hydrogène. La position des atomes d'hydrogène a été déterminée directement, et un schéma vraisemblable des liaisons hydrogène a été établi. Nous évaluons la connectivité des chaînes (Beφ_4–$T\varphi_4$) (*T* = Si,P) dans les minéraux de Be, et nous l'utilisons pour dresser une hiérarchie selon la complexité topologique.

(Traduit par la Rédaction)

Mots-clés: väyrynenite, affinement de la structure, analyse à la microsonde électronique, minéraux de Be.

INTRODUCTION

The structure of väyrynenite, (Mn^{2+},Fe^{2+})Be(PO_4)(OH), was determined by Mrose & Appleman (1962); it has a structure similar to that of euclase, $AlBe(SiO_4)(OH)$. Mrose & Appleman (1962) emphasized the electronic differences between a structure containing Mn^{2+} and P and a structure containing Al and Si. In fact, there is a significant topological difference between the chains in these two minerals. The structure of väyrynenite has been refined to locate the position of the H atom, to establish the stereochemical details of the H-bonding arrangement, and to further examine aspects of chain connectivity in Be minerals.

EXPERIMENTAL

The specimen of väyrynenite used here is from Sassi, Gilgit Skardu Road area, Pakistan, and is commonly associated with other Be minerals such as herderite and

§ *E-mail address*: frank_hawthorne@umanitoba.ca

TABLE 1. MISCELLANEOUS REFINEMENT DATA FOR VÄYRYNENITE

a (Å)	5.4044(6)	Radiation	Mo*K*α/graphite
b	14.5145(12)	Total no. of *I*	2116
c	4.7052(6)	No. of $\|F\|$	1063
β (°)	102.798(9)	No. of $\|F_o\| > 5\sigma$	1001
V (Å^3)	359.91(7)	*R*(merge) %	1.4
Space group	$P2_1/a$	*R*(obs) %	1.5
Z	4	*wR*(obs)%	1.8
μ (mm^{-1})	4.00		

$R = \Sigma(|F_o|-|F_c|)/\Sigma|F_o|$

$wR = [\Sigma w(|F_o|-|F_c|)^2/\Sigma F_o^2]^{1/2}$, $w = 1$

beryllonite. The crystals are transparent and light pink in color. The crystal used to collect single-crystal X-ray diffraction and electron-microprobe data was ground to a 0.10 × 0.14 × 0.16 mm spheroid and mounted on a tapered glass rod.

X-ray diffraction

The unit-cell dimensions were determined using a Siemens *P*4 automated four-circle diffractometer with a graphite monochromator and a Mo*K*α X-ray tube. Twenty-five reflections between 7 and 30°2θ were centered, and a constrained monoclinic cell was determined from the setting angles and refined using least-squares (Table 1). Single-crystal intensity data were measured from 4 to 60°2θ over two octants with a scan range of 1.2° and scan-speeds from 2.5 to 29.3°/min. A total of 2203 intensities was measured over one asymmetric unit. Psi-scan data were measured on 20 reflections out to 60°2θ at increments of 5°, and an absorption correction, modeling the crystal as a triaxial ellipsoid, reduced *R*(azimuthal) from 1.8 to 0.8%. Intensities were corrected for Lorentz, polarization and background effects, and then reduced to structure factors; of the 1063 unique reflections, 1001 were classed as observed ($|F_o| > 5\sigma F$).

TABLE 2. CHEMICAL COMPOSITION (wt%) AND UNIT FORMULA (*apfu*)* FOR VÄYRYNENITE

MnO	30.88	Mn^{2+}	0.776
FeO	9.37	Fe^{2+}	0.229
MgO	0.17	Mg	0.007
P_2O_5	40.25	Σ	1.012
BeO†	14.22		
H_2O†	4.71	P	0.988
F	0.86		
O = F	–0.36	Be	1.000
Sum	100.10		
		OH**	0.920
		F	0.080
		Σ	1.000

* Calculated based on 5 anions *pfu*
** Calculated assuming OH + F = 1.00 *apfu*
† Determined by stoichiometry

Chemical analysis

The same crystal used for X-ray diffraction was mounted in a perspex disc, ground, polished and coated with carbon for chemical analysis using a Cameca SX–50 electron microprobe. The crystal was analyzed for Fe, Mn, Mg, Si and F in wavelength-dispersion mode. Ten points were analyzed with the following conditions: excitation voltage: 15 kV; specimen current: 20 nA; beam size: 5 μm; peak count time: 2 s; background count time: 10 s. The following standards and crystals were used (*K*α X-ray lines): F: fluororiebeckite, TAP; Mg: forsterite; TAP; Al: andalusite, TAP; Si: diopside, PET/TAP; P: maricite, PET; Mn: spessartine, LiF; Fe: maricite, LiF. The resulting chemical composition and unit formula are given in Table 2; the BeO and H_2O contents were calculated on the basis of stoichiometry.

Crystal-Structure Refinement

All calculations were done with the SHELXTL PC Plus system of programs; *R* indices are of the form given in Table 1, and are expressed as percentages. Refinement was initiated with the atom coordinates of Mrose & Appleman (1962), and refinement converged to an

TABLE 3. ATOM COORDINATES AND DISPLACEMENT PARAMETERS FOR VÄYRYNENITE

Site	*x*	*y*	*z*	U_{eq}*	U_{11}	U_{22}	U_{33}	U_{23}	U_{13}	U_{12}
Mn	0.24887(4)	0.43928(2)	0.93894(5)	0.0084(1)	0.0064(1)	0.0082(1)	0.0102(1)	–0.0009(1)	0.0010(1)	0.0004(1)
P	0.19518(7)	0.10456(3)	0.54042(8)	0.0062(1)	0.0062(2)	0.0059(2)	0.0062(2)	–0.0002(1)	0.0008(1)	0.0000(1)
Be	0.4369(4)	0.2625(1)	0.7811(4)	0.0087(5)	0.0085(8)	0.0089(8)	0.0087(8)	0.0002(7)	0.0023(7)	–0.0002(7)
O(1)	0.3658(2)	0.03931(8)	0.7548(3)	0.0098(3)	0.0079(5)	0.0099(5)	0.0108(5)	0.0032(4)	0.0006(4)	0.0008(4)
O(2)	0.4608(2)	0.36598(7)	0.6591(2)	0.0086(3)	0.0078(5)	0.0075(5)	0.0112(5)	0.0002(4)	0.0038(4)	–0.0007(4)
O(3)	0.3440(2)	0.19313(8)	0.5101(2)	0.0090(3)	0.0104(5)	0.0078(5)	0.0087(5)	–0.0007(4)	0.0023(4)	–0.0032(4)
O(4)	0.1045(2)	0.05938(8)	0.2441(2)	0.0093(3)	0.0101(5)	0.0093(5)	0.0078(5)	–0.0023(4)	0.0007(4)	–0.0002(4)
O(5)	0.2122(2)	0.27691(8)	0.9691(2)	0.0086(3)	0.0076(5)	0.0106(5)	0.0075(5)	0.0005(4)	0.0013(4)	–0.0004(4)
H	0.256(5)	0.252(2)	1.168(2)	0.0340(74)						

R-index of 1.7% for anisotropic-displacement parameters. At this stage of the refinement, a difference-Fourier map was calculated, and the coordinates of the H position were determined. It is well known that refinement of H positions using X-ray intensity data results in anomalously short O–H bond-lengths because the center of gravity of the electron density associated with the H atom is moved significantly toward the donor O atom by chemical bonding. Thus a soft constraint was imposed on the refinement (whereby the O–H distance should be ~0.98 Å) by adding extra weighted observational equations to the least-squares matrix. Only the O–H distance is constrained, and the H position is free to seek its optimal position around the O atom. Refinement of all parameters converged to a final *R* index of 1.5%. Final atom positions and displacement parameters are given in Table 3, selected interatomic distances and angles are listed in Table 4, and bond valences are given in Table 5. Observed and calculated structure-factors may be obtained from the Depository of Unpublished Data, CISTI, National Research Council of Canada, Ottawa, Ontario K1A 0S2, Canada.

TABLE 4. SELECTED INTERATOMIC DISTANCES (Å) AND ANGLES (°) FOR VÄYRYNENITE

M–O(1)a	2.228(1)	O(1)–*P*–O(3)	109.1(1)
M–O(1)b	2.083(1)	O(1)–*P*–O(2)b	110.7(1)
M–O(2)	2.201(1)	O(1)–*P*–O(4)	111.2(1)
M–O(4)d	2.170(1)	O(3)–*P*–O(2)b	106.7(1)
M–O(4)e	2.129(1)	O(3)–*P*–O(4)	110.1(1)
M–O(5)	2.372(1)	O(4)–*P*–O(2)b	109.0(1)
<*M*–O>	2.197	<O–*P*–O>	109.5(1)
P–O(1)	1.534(1)	O(2)–*Be*–O(3)	109.4(1)
P–O(2)b	1.553(1)	O(2)–*Be*–O(5)	101.3(1)
P–O(3)	1.540(1)	O(2)–*Be*–O(5)f	112.1(1)
P–O(4)	1.520(1)	O(3)–*Be*–O(5)	111.2(1)
<*P*–O>	1.537	O(3)–*Be*–O(5)f	107.0(1)
		O(4)–*Be*–O(5)f	115.7(1)
Be–O(1)a	1.623(2)	<O–*Be*–O>	109.5(1)
Be–O(1)b	1.615(2)		
Be–O(2)	1.666(3)	O(5)–*M*–O(1)	124.7(1)
Be–O(4)d	1.655(2)	O(5)–*M*–O(4)	92.5(1)
<*Be*–O>	1.640	O(5)–*M*–O(2)	67.5(1)
		O(5)–*M*–O(1)	94.8(1)
		O(4)–*M*–O(2)	82.3(1)
O(5)–H···O(3)	172(2)	O(4)–*M*–O(1)b	97.6(1)
O(5)–H	0.98(1)	O(4)–*M*–O(1)a	84.9(1)
O(3)···H	1.79(1)	O(4)–*M*–O(4)e	84.6(1)
		O(1)–*M*–O(1)b	77.2(1)
		O(1)–*M*–O(4)e	84.1(1)
		O(4)–*M*–O(2)	84.0(1)
		O(2)–*M*–O(1)	115.1(1)

Symmetry operators: a: $\bar{x}$ + ½, *y* + ½, *z* + ½; b: *x* – ½, $\bar{y}$ + ½, *z*; c: *x*, *y*, *z* + 1; d: $\bar{x}$ + ½, *y* + ½, $\bar{z}$ + 1; e: *x* + ½, $\bar{y}$ + ½, *z* + 1; f: *x* + ½, $\bar{y}$ + ½, *z*.

TABLE 5. EMPIRICAL BOND-VALENCES (*vu*) FOR VÄYRYNENITE

	M	*P*	*Be*	H	Σ
O(1)	0.31	1.25			2.01
	0.45				
O(2)	0.33	1.19	0.52		2.04
O(3)		1.23	0.53	0.20	1.96
O(4)	0.36	1.30			2.06
	0.40				
O(5)	0.21		0.46	0.80	1.95
			0.48		
Σ	2.06	4.97	1.99	1.00	

*Bond valences calculated using the curves of Brown & Altermatt (1985).

Description of the Structure

Cation polyhedra

In the structure of väyrynenite, there is one *Be* site surrounded by two hydroxyl groups and two O atoms in a tetrahedral arrangement. The <*Be*–O> distance of 1.640 Å is close to the grand <Be–O> distance of 1.633 Å given by Hawthorne & Huminicki (2001) for Be minerals. However, the ($Be\varphi_4$) tetrahedron has an individual bond-length variation of 0.051 Å. Inspection of Table 5 shows the origin of the distortion. The *Be* site is coordinated by O(2), O(3) and two O(5) anions. The O(2) and O(3) anions are both [3]-coordinated (by *M, P* and *Be,* and by *P, Be* and H, respectively), whereas the oxygen atom of the O(5) anion is [4]-coordinated (by *M*, *Be* × 2 and H). In order for the sum of the bond valences incident at O(5) to be close to the ideal value of 2 valence units (*vu*), the *Be*–O(5) bond-valences have to be significantly less than 0.5 *vu* each, thus forcing the *Be*–O(5) distances to be significantly longer than the <*Be*–O> distance (which corresponds to a bond valence of 0.5 *vu*). There is one *P* site coordinated by four O atoms in a tetrahedral arrangement, and the <P–O> distance of 1.537 Å is identical to the grand <P–O> distance of 1.537 Å given by Baur (1974).

There is one *M* site occupied by Mn + Fe + Mg and surrounded by six anions in an octahedral arrangement, with one bond [to the O(5) anion] being significantly longer than the others. The distortion of the ($M\varphi_6$) octahedron is easily apparent in Figure 1; the *M*–O(5) bond is strongly elongate relative to the other *M*–O bonds, and some of the O–*M*–O(5) bond angles deviate considerably from their ideal values of 90° (Table 4). In order to satisfy the valence-sum rule (Table 5), the O(5) anion acquires 0.46 and 0.48 *vu* from two Be atoms and 0.8 *vu* from the H atom; the bond valence required from the *M*-site cation is ~0.25 *vu*. The average bond-valence for an Mn–O bond is ~0.33 *vu*, and hence the *M*–O(5) bond length will be considerably larger than the mean bond-length (Table 4). Inspection of Table 4 shows that the O(1)–*M*–O(5) and O(2)–*M*–O(5) angles (124.7 and 67.5°, respectively) depart considerably from the ideal value of 90° for a holosymmetric octahedron. Figure 1

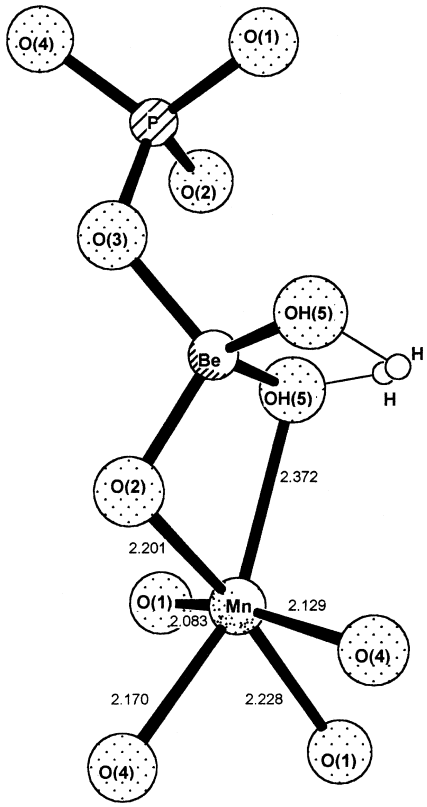

FIG. 1. The coordination polyhedra in väyrynenite, showing the distortion of the ($M\varphi_6$) octahedron and the location of the H atom.

shows that the ($M\varphi_6$) octahedron shares an edge with the ($Be\varphi_4$) tetrahedron. The mean edge-length of the ($Be\varphi_4$) tetrahedron, 2.678 Å, is much less than the mean edge-length of the ($M\varphi_6$) octahedron, 3.185 Å. However, where a ($Be\varphi_4$) tetrahedron and an ($M\varphi_6$) octahedron have a common edge, the polyhedra must distort from their holosymmetric configurations. Inspection of the bond lengths and angles of the two polyhedra involved (Table 4) shows that nearly all of the distortion required for this edge-sharing configuration occurs in the ($M\varphi_6$) octahedron, specifically by adoption of a very small (67.5°) O(2)–*M*–O(5) angle. This is the origin of the prominent angular distortion of the ($M\varphi_6$) octahedron in väyrynenite.

The refined scattering value at the *M* site is 25.0 *epfu* (electrons per formula unit). The analogous value calculated from the results of the electron-microprobe analysis and normalized to a site occupancy of 1.0 is 25.1 *epfu.* These values are extremely close; the population of the *M* site is considered to be that indicated by the unit formula (Table 2) calculated from the electron-microprobe analysis.

Hydrogen bonding

The H atom, located in the difference-Fourier map and refined using soft constraints, is strongly bonded to the O(5) anion. Ignoring the H atom, the sum of the bond valences around O(5) is 1.15 *vu* (Table 5). Hence, the H atom must bond to O(5) in order to bring its incident bond-valence sum close to the required value of 2 *vu,* confirming the results of the refinement. The H atom will also bond weakly to an acceptor anion, forming a hydrogen bond (Baur 1972). In the case of väyrynenite, the hydrogen-bond acceptor is O(3), based on bond-valence relations and bond distances.

Structure topology

Beryllium minerals with infinite chains of ($T\varphi_4$) tetrahedra can be divided into two groups based on the types of linkages in the chains: (1) structures with Be–Si (and Si–Si) linkages, and (2) structures with Be–P (and Be–As) linkages. Väyrynenite is in the second category, as it contains ($P\varphi_4$) groups rather than ($Si\varphi_4$) groups. It has been noted that there is only minor hydrogen bonding in minerals of the first category, whereas there is extensive hydrogen bonding in minerals of the second category (Hawthorne & Huminicki 2001).

Each ($Be\varphi_4$) tetrahedron connects by corner-sharing to form a chain that extends in the *a* direction. This chain is decorated along its periphery by (PO_4) tetrahedra that share corners with ($Be\varphi_4$) tetrahedra to form ribbons that extend along the *a* axis (Fig. 2). These $[Be_2(OH)_2(PO_4)_2]^{4n-}$ ribbons are linked in the *b* direction by (Mn^{2+}, Fe^{2+}) in octahedral coordination. The resultant (001) sheets are linked to other sheets in the *c* direction by corner-sharing of O-atoms between (PO_4) tetrahedra and ($M\varphi_6$) octahedra, and by hydrogen bonds (Fig. 3).

COMPARISON TO RELATED STRUCTURES

Mrose & Appleman (1962) commented on the similarity of the beryllophosphate chain in väyrynenite (Fig. 2) and the beryllosilicate chain in euclase (Fig. 4). Although these chains consist of a central corner-sharing chain of ($Be\varphi_4$) tetrahedra flanked by phosphate or silicate tetrahedra, there is a major topological difference between the two chains: in the väyrynenite chain (Fig. 2), all linking anions are [2]-coordinated, whereas in the euclase chain, the linking anions are both [2]-coordinated and [3]-coordinated. This difference in tetrahedron connectivity is more clearly seen if the chains are represented as graphs (Hawthorne 1983, 1994, 1997). In Figure 5, the chains occurring in all *Be* minerals based on ($Be\varphi_4$)–($T\varphi_4$) chain linkages (Hawthorne & Huminicki 2001) are represented as graphs; solid and hollow circles (nodes) represent ($Be\varphi_4$) and ($T\varphi_4$) tetrahedra, respectively, and lines (edges) denote corner-linkage between tetrahedra. The difference between the

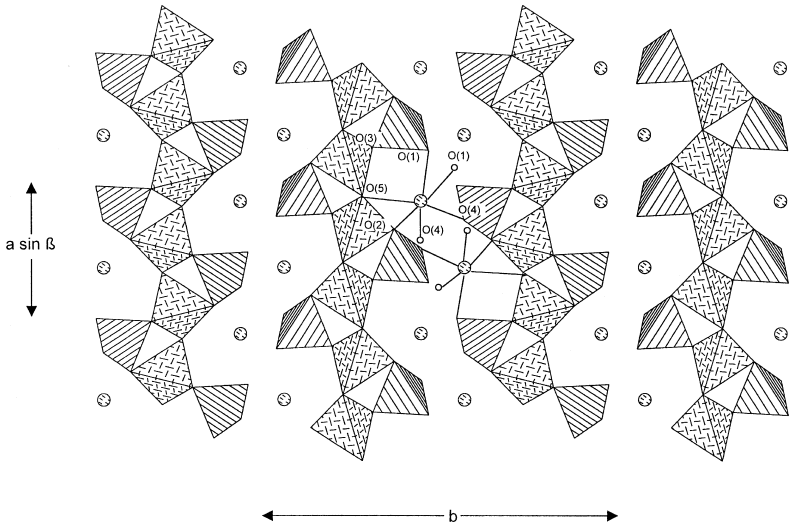

FIG. 2. Väyrynenite projected down the *c* axis. Chains of ($Be\varphi_4$) tetrahedra (cross-hatched) are linked by corner-sharing of O(5) atoms and are flanked on the sides by (PO_4) tetrahedra (lined). *M* cations in octahedral coordination are shown interstitially as hatched circles.

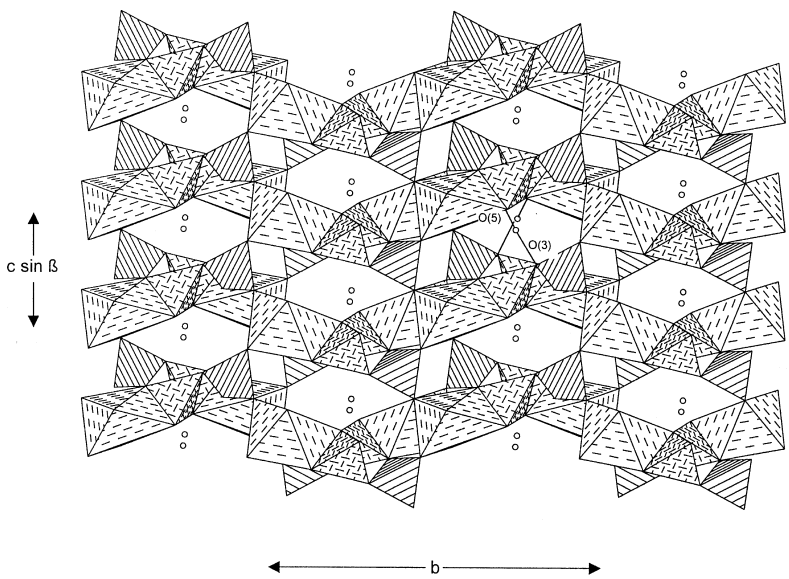

FIG. 3. Väyrynenite projected onto (100). The H atoms are located between the sheet that repeats along the (100) plane, and are bonded to O(5) that bridges to other Be tetrahedra in the *a* direction. There is a hydrogen bond to O(3) (narrow line).

chains in väyrynenite and euclase is immediately apparent in this graphical representation: in väyrynenite, the ($Be\varphi_4$) tetrahedra are four-connected and the ($T\varphi_4$) tetrahedra are two-connected, whereas in euclase, the ($Be\varphi_4$) tetrahedra are five-connected and the ($T\varphi_4$) tetrahedra are three-connected.

($Be\phi_4$)–($T\phi_4$) Chains in Minerals

Figure 5 shows graphs of the ($Be\varphi_4$)–($T\varphi_4$) chains in minerals, arranged in terms of increasing complexity and connectivity. There are no simple linear chains of the form [(Be,*T*)φ_3]. Khmaralite, [$(Mg,Fe^{2+})_7(Al,Fe^{3+})_9$]($Al_6Be_{1.5}Si_{4.5}$)$O_{40}$ [Barbier *et al.* (1999)], "makarochkinite" – a natural material with the aenigmatite structure, $Ca_2Fe^{2+}{}_4Fe^{3+}Ti^{4+}O_2[BeAlSi_4O_{18}]$ [Yakubovich *et al.* (1990)], and surinamite, $Mg_3Al_4[BeSi_3O_{16}]$ [Moore & Araki (1983)], all consist of branched variants of the [(Be,*T*)φ_3] chain: a central [(Be,*T*)φ_3] backbone is decorated by additional ($T\varphi_4$) tetrahedra (Fig. 5). Surinamite has a backbone consisting of alternating (Beφ_4) and triplets of ($T\varphi_4$) tetrahedra, khmaralite has a backbone of alternating (Beφ_4) and pairs of ($T\varphi_4$) tetrahedra, and "makarochkinite" has a backbone of alternating (Beφ_4) tetrahedra and triplets of ($T\varphi_4$) tetrahedra. Surinamite has a ratio of backbone to decorating tetrahedra of 4:1, whereas khmaralite and "makarochkinite" have analogous ratios of 4:2. Within this general theme, there are numerous other possibilities for fairly simply connected (Beφ_4)–($T\varphi_4$) chains.

Väyrynenite (Fig. 5) also has a backbone of the general form [XO_3], but unlike khmaralite, "makarochkinite" and surinamite, it consists solely of (Beφ_4) tetrahedra. It is decorated on either side by ($T\varphi_4$) tetrahedra, but unlike the previous chains [Fig. 5, (1)–(3)], the ($T\varphi_4$) tetrahedra connect to two (Beφ_4) tetrahedra, rather than one. Sverigite, $NaMn^{2+}{}_2Sn^{4+}[Be_2Si_3O_{12}(OH)]$ [Rouse *et al.* (1989)], has a [(Be_3T)φ_3] backbone in which the Be:*T* ratio is 2:1. The backbone is decorated by (Beφ_4) tetrahedra that link the (Beφ_4) tetrahedra separated by the ($T\varphi_4$) tetrahedra [*i.e.*, such that these are four-membered rings of tetrahedra joined *via* corner-linked (Beφ_4) tetrahedra]. Fransoletite, $Ca_3[Be_2(PO_4)_2(PO_3\{OH\})_2](H_2O)_4$ [Kampf (1992)], has a [(Be,*T*)φ_3] backbone topologically and topochemically identical to that in surinamite: alternating corner-linked (Beφ_4) and ($T\varphi_4$) tetrahedra. However, the linkage of the decorating tetrahedra is far more complicated than in surinamite: ($T\varphi_4$) tetrahedra link (Beφ_4) tetrahedra separated by a ($T\varphi_4$) tetrahedron, similar to the decorating linkage in sverigeite. However, in fransoletite, all backbone linkages are spanned by a decorating linkage, whereas in sverigeite, adjacent (Beφ_4) tetrahedra are not spanned by a decorating linkage. Euclase (Fig. 5) has a [Beφ_3] backbone decorated by ($T\varphi_4$) tetrahedra, but unlike the chains in väyrynenite, the ($T\varphi_4$) tetrahedra link to three (Beφ_4) tetrahedra [rather than the two ($Be\varphi_4$) tetrahedra in väyrynenite]. The result is a more connected chain in euclase.

The remaining chains are somewhat more complicated, and we can represent them in two ways (Fig. 5): on the left, we show the graph of the chain retaining the analogous spatial relations of the tetrahedra, whereas on the right, we show the chains in the form of a central backbone plus decorations. In joesmithite, $Pb^{2+}Ca_2(Mg_3Fe^{3+}{}_2)[Be_2Si_6O_{22}](OH)_2$ [Moore *et al.* (1993)], the chains consist of two [(Be,*T*)φ_3] chains cross-linked at alternate vertices (tetrahedra); this is actually the amphibole chain. Alternatively, we can represent it as a

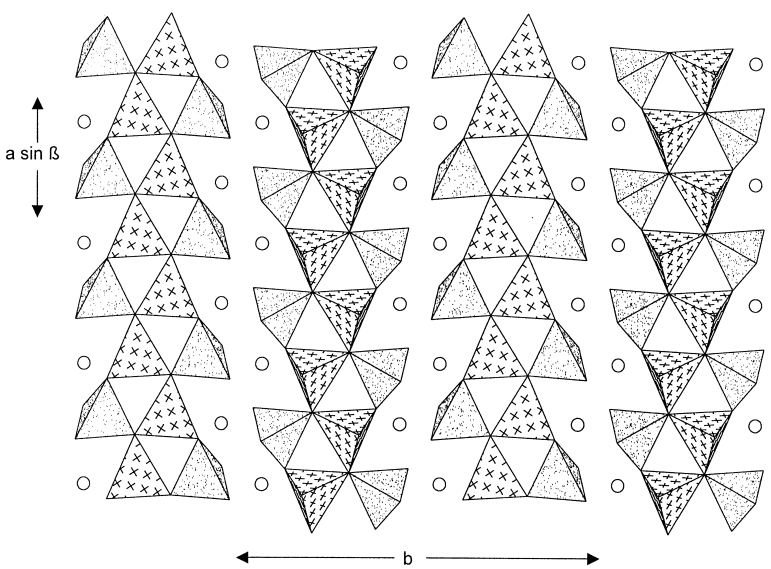

FIG. 4. Euclase projected down the *c* axis. Chains consist of (Beφ_4) (crosses) and (Siφ_4) (dotted) with cross-linking (Alφ_6) octahedra (interstitial circles) similar to väyrynenite.

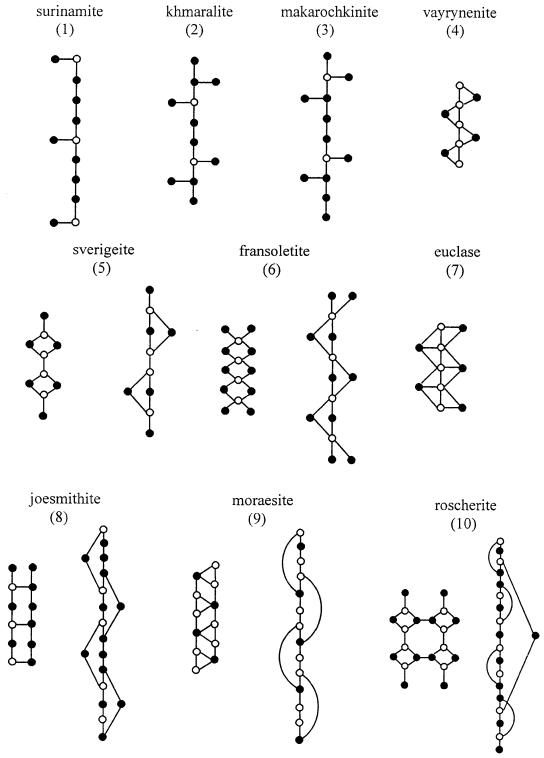

FIG. 5. Graphical representation of (Beφ_4)–($T\varphi_4$) chains in Be-bearing minerals; hollow circles are (Beφ_4) tetrahedra, solid circles are other ($T\varphi_4$) tetrahedra, and the lines connecting the circles indicate corner-linkage between tetrahedra.

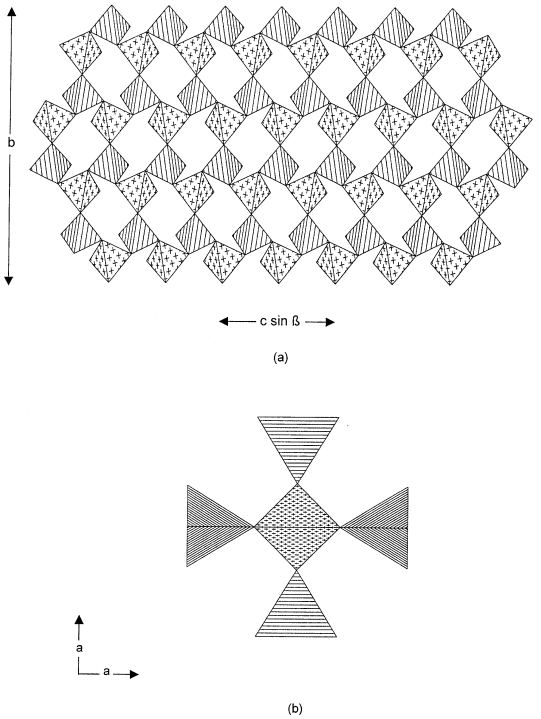

FIG. 6. Be–P linkages for (a) the beryllophosphate framework structure of babefphite and (b) the cluster for gainesite. The (BeO_4) tetrahedra have a cross pattern, and the (PO_4) tetrahedra are indicated with dashed lines.

single [(Be,T)φ_3] backbone decorated by ($T\varphi_4$) tetrahedra that link selected vertices four tetrahedra apart. In moraesite, $[Be_2PO_4(OH)](H_2O)_4$ [Merlino & Pasero (1992)], the chain consists of two [(Be,T)φ_3] chains with cross-linking between ($Be\varphi_4$) and ($T\varphi_4$) tetrahedra. Alternatively, the chain can be represented as a single [(Be,T)φ_3] backbone with links between tetrahedra that are not adjacent along the length of the backbone chain. We can designate this kind of linkage as *looping*. Roscherite, $Ca_2Mn^{2+}{}_5[Be_4P_6O_{24}(OH)_4(H_2O)_6$ [Fanfani *et al.* (1975, 1977)], has the most complex chains. They can be thought of as two sverigeite-type chains cross-linked through adjacent ($T\varphi_4$) tetrahedra (Fig. 5). Alternatively, they may be considered as a [(Be,T)φ_3] backbone decorated by ($T\varphi_4$) tetrahedra linking (Beφ_4) tetrahedra that are separated by twelve tetrahedra along the backbone, and also showing looping between selected (Beφ_4) and ($T\varphi_4$) tetrahedra four tetrahedra apart along the chain.

In addition to clarifying the character of tetrahedron connectivity in the chains occurring in the Be minerals, this graphical representation of chains suggests a systematic way of investigating chain connectivity. All of the chains in Figure 5 can be considered as backbone [$T\varphi_3$] chains (T = Be, Al, Si, P, *etc.*) that are modified by decoration or by looping (or both). Thus, topological derivation of all possible chain configurations seems possible using such an approach.

There are nineteen known beryllophosphate structures that occur in Nature, together with a few synthetic beryllophosphates. All these structures have corner-sharing linkages of ($Be\varphi_4$) and ($P\varphi_4$) tetrahedra. Only three known beryllophosphate structures do not consist of four-membered rings of corner-sharing ($Be\varphi_4$)–($P\varphi_4$) tetrahedra: the chain structure of väyrynenite, the framework structure of babefphite [Ba(BePO$_4$F), Simonov *et al.* 1980] (Fig. 6a), and the cluster structure of gainesite [$NaKZr_2(BePO_4O_{16})$, Moore *et al.* 1983] (Fig. 6b). Väyrynenite is the only known beryllophosphate that has a ($Be\varphi_4$)–($P\varphi_4$) linkage that does not consist of alternating ($Be\varphi_4$) and ($P\varphi_4$) tetrahedra but rather forms chains of three-membered ($Be\varphi_4$)–($Be\varphi_4$)–($P\varphi_4$) rings linked through common (Beφ_4) tetrahedra (Kampf 1992).

ACKNOWLEDGEMENTS

We thank Mark Cooper for help with data collection, and Jacques Barbier and Olga Yakubovich for their comments on the manuscript. This work was funded by Natural Sciences and Engineering Research Council of Canada grants to FCH.

REFERENCES

BARBIER, J., GREW, E.S., MOORE, P.B. & SU, SHU-CHUN (1999): Khmaralite, a new beryllium-bearing mineral related to sapphirine: a superstructure resulting from partial ordering of Be, Al, and Si on tetrahedral sites. *Am. Mineral.* **84**, 1650-1660.

BAUR, W.H. (1972): Prediction of hydrogen bonds and hydrogen atom positions in crystalline solids. *Acta Crystallogr.* **B28**, 1456-1465.

_____ (1974): The geometry of polyhedral distortions. Predictive relationships for the phosphate group. *Acta Crystallogr.* **B30**, 1195-1215.

BROWN, I.D. & ALTERMATT, D. (1985): Bond-valence parameters obtained from a systematic analysis of the inorganic crystal structure database. *Acta Crystallogr.* **B41**, 244-247.

FANFANI, L., NUNZI, A., ZANAZZI, P.F. & ZANZARI, A.R. (1975): The crystal structure of roscherite. *Tschermaks Mineral. Petrogr. Mitt.* **22**, 266-277.

_____, ZANAZZI, P.F. & ZANZARI, A.R. (1977): The crystal structure of a triclinic roscherite. *Tschermaks Mineral. Petrogr. Mitt.* **24**, 169-178.

HAWTHORNE, F.C. (1983): Graphical enumeration of polyhedral clusters. *Acta Crystallogr.* **A39**, 724-736.

_____ (1994): Structural aspects of oxide and oxysalt crystals. *Acta Crystallogr.* **B50**, 481-510.

_____ (1997): Short-range order in amphiboles: a bond-valence approach. *Can.Mineral.* **35**, 203-218.

_____ & HUMINICKI, D.M.C. (2001): The crystal chemistry of beryllium. *Rev. Mineral.* (in press).

KAMPF, A.R. (1992): Beryllophosphate chains in the structures of fransoletite, parafransoletite, and ehrleite, and some general comments on beryllophosphate linkages. *Am. Mineral.* **77**, 848-856.

MERLINO, S. & PASERO, M. (1992): Crystal chemistry of beryllophosphates: the crystal structure of moraesite, $Be_2(PO_4)(OH)\cdot 4H_2O$. *Z. Kristallogr.* **201**, 253-262.

MOORE, P.B. & ARAKI, T. (1983): Surinamite, *ca.* $Mg_3Al_4Si_3BeO_{16}$: its crystal structure and relation to sapphirine, *ca.* $Mg_{2.8}Al_{7.2}Si_{1.2}O_{16}$. *Am. Mineral.* **68**, 804-810.

_____, _____, STEELE, I.M., SWIHART, G.H. & KAMPF, A.R. (1983): Gainesite, sodium zirconium beryllophosphate: a new mineral and its crystal structure. *Am. Mineral.* **68**, 1022-1028.

_____, DAVIS, A.M., VAN DERVEER, D.G. & SEN GUPTA, P.K. (1993): Joesmithite, a plumbous amphibole revisited and comments on bond valences. *Mineral. Petrol.* **48**, 97-113.

MROSE, M.E. & APPLEMAN, D.E. (1962): The crystal structures and crystal chemistry of väyrynenite, (Mn, Fe)$Be(PO_4)(OH)$, and euclase, $AlBe(SiO_4)(OH)$. *Z. Kristallogr.* **117**, 16-36.

ROUSE, R.C., PEACOR, D.R. & METZ, G.W. (1989): Sverigeite, a structure containing planar NaO_4 groups and chains of 3- and 4-membered beryllosilicate rings. *Am. Mineral.* **74**, 1343-1350.

SIMONOV, M.A., EGOROV-TISMENKO, Y.K. & BELOV, N.V. (1980): Use of modern X-ray equipment to solve fine problems of structural mineralogy by the example of the crystal structure of babefphite $BaBe(PO_4)F$. *Sov. Phys. Crystallogr.* **25**, 28-30.

YAKUBOVICH, O.V., MALINOVSKII, YU.A. & POLYAKOV, V.O. (1990): Crystal structure of makarochkinite. *Sov. Phys. Crystallogr.* **35**, 818-822.

Received June 20, 2000, revised manuscript accepted October 11, 2000.